Electronic Supplementary Material (ESI) for Metallomics.

The pivotal role of MBD4-ATP7B in the human Cu(I) excretion path as revealed by EPR experiments and all-atom simulations

Zena Qasem†[,a], Matic Pavlin†[,b], Ida Ritacco[b], Lada Gevorkyan-Airapetov[a], Alessandra Magistrato[*,b] and Sharon Ruthstein[*,a]

Supporting Information

Scheme S1
Figure S1-S9
Tables S1-S3

[a.] *Chemistry Department, Faculty of Exact Sciences, Bar-Ilan University, Israel 529002.*
[b.] *CNR-IOM at SISSA, via Bonomea 265, 34135, Trieste, Italy.*
† These authors contributed equally to this work.
* Corresponding authors: Sharon.ruthstein@biu.ac.il; alessandra.magistrato@sissa.it .

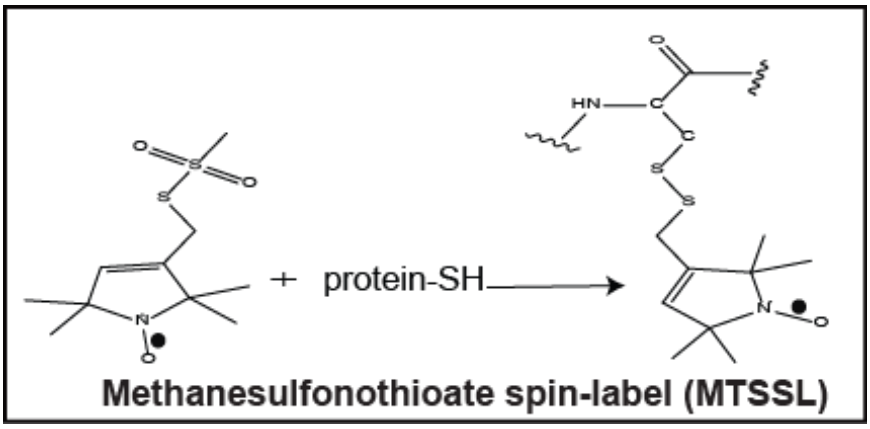

Scheme S1: Spin-labeling reaction with MTSSL

DEER experiments

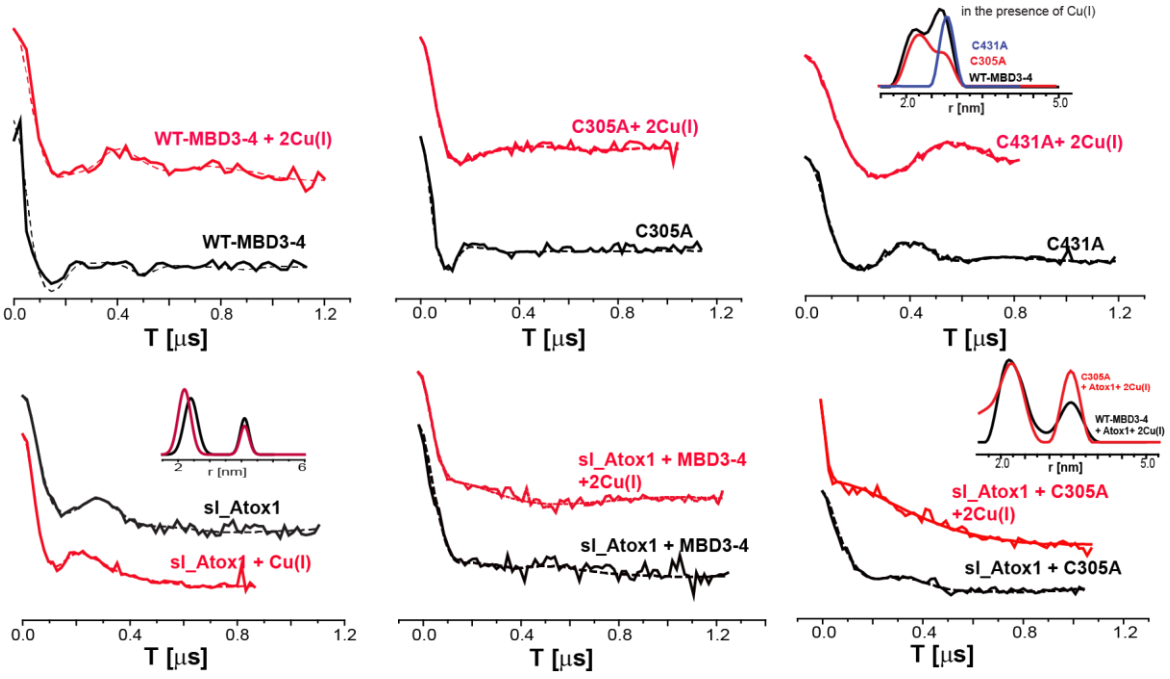

Figure S1: DEER Raw data.

Continuous Wave (CW)-EPR experiments

CW-EPR spectra were recorded using an E500 Elexsys Bruker spectrometer operating at 9.0–9.5 GHz equipped with a super-high-sensitivity CW resonator. The spectra were recorded at room temperature (292 ± 5 K) at a microwave power of 20.0 mW, a modulation amplitude of 1.0 G, a time constant of 60 ms, and a receiver gain of 60.0 dB. The samples were measured in 1.0-mm quartz tubes (Wilmad-LabGlass, Vineland, NJ). CW-EPR simulations were carried out using MATLAB, with the EasySpin toolbox.[1]

CW-EPR experiments can derive the dynamics of the spin labels attached to the protein chains. CW-EPR spectra support the DEER signal presented in Figure S1. The CW-EPR spectra were best simulated with two dynamic species, where the dominant species was simulated with the addition of a nearby spin label with a 5 MHz dipolar interaction (corresponding to a distance of ~2.2 nm). The extent of this species changes upon Cu(I) and Atox1 binding. A reduction in the contribution of this dominant species was observed both for WT-MBD3-4, as well as for the two mutants: MBD3-4_C305A and MBD3-4_C431A (see Figure S2 and Table S1). This results in larger average distances between spin labels upon Cu(I) binding. In addition, an increase in dynamics, specifically for MBD3-4_C305A was observed, which agreed well with the wider distance distribution obtained for MBD3-4_C305A + Cu(I).

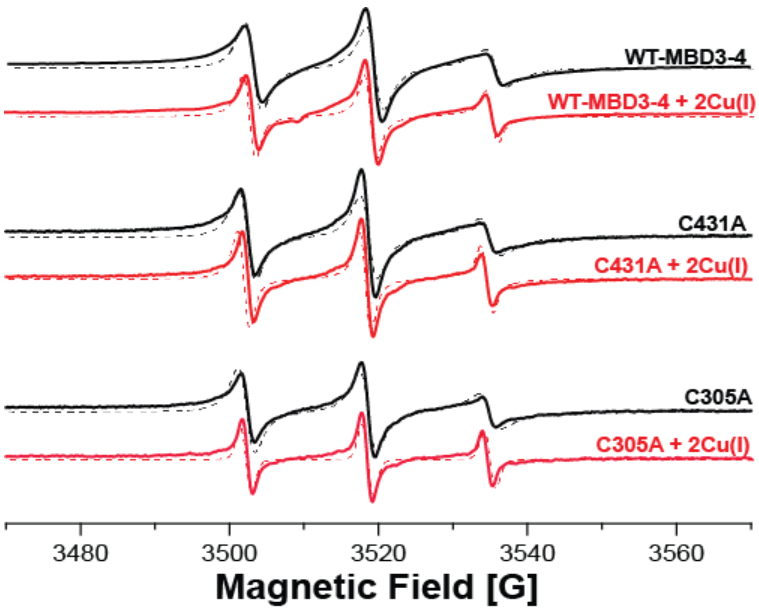

Figure S2: CW-EPR spectra for WT-MBD3-4, MBD3-4_C431A mutant, and MBD3-4_C305A mutant, in the absence (black line) and presence (red line) of Cu(I). The dashed lines are simulated spectra.

Table S1: Simulated parameters for CW-EPR spectra obtained with easyspin, chili method, in the presence of two species at a g tensor of [2.0087 2.006 2.0022].

Sample	**A-tensor [MHz] (± 0.5 MHz)**	**τ (correlation time (sec)) (± $0.05 \cdot 10^{-9}$)**	**Exchange/Dipolar interaction [MHz] (± 0.1 MHz)**	**% species (± 0.05%)**
Sl_WT_MBD3-4	[25 25 90]	$1 \cdot 10^{-9}$	5.0	98%
	[25 25 86]	$1 \cdot 10^{-9}$	0.0	2%
Sl_WT_MBD3-4 + Cu(I)	[25 25 90]	$1 \cdot 10^{-9}$	5.0	85%
	[25 25 88]	$0.6 \cdot 10^{-10}$	0.0	15%
C431A	[25 25 90]	$1 \cdot 10^{-10}$	5.0	98%
	[25 25 86]	$1 \cdot 10^{-9}$	0.0	2%
C431A+Cu(I)	[25 25 90]	$1 \cdot 10^{-9}$	5.0	80%
	[25 25 88]	$0.6 \cdot 10^{-10}$	0.0	20%
C305A	[25 25 90]	$1 \cdot 10^{-9}$	5.0	98%
	[25 25 86]	$1 \cdot 10^{-9}$	0.0	2%
C305A+Cu(I)	[25 25 90]	$1 \cdot 10^{-9}$	5.0	30%
	[25 25 88]	$0.6 \cdot 10^{-10}$	0.0	70%
Atox1+Cu(I)	[25 25 90]	$1 \cdot 10^{-9}$	5.0	85%
	[25 25 88]	$0.6 \cdot 10^{-10}$	0.0	15%
Sl-Atox1+MBD34+Cu(I)	[25 25 90]	$1 \cdot 10^{-9}$	5.0	85%
	[25 25 88]	$0.6 \cdot 10^{-10}$	0.0	15%

CW-EPR spectra were also recorded in the presence of Atox1 and spin-labeled Atox1 (labeled at C41 position and termed sl-Atox1). Figure S3A shows the various spectra, where sl-MBD34 corresponds to spin-labeled WT-MBD3-4, and MBD34 corresponds to non-spin-labeled WT-MBD3-4. The spectra indicate two interesting features. The first one when MBD3-4 is added to a spin-labeled Atox1+Cu(I) solution, a transition from Atox1 dimer to Atox1 monomer occurs, manifested by a reduction in exchange interaction, and an increase in mobility. The second

feature is that when adding either sl-Atox1 or Atox1 to sl-WT-MBD3-4 + Cu(I) solution, no change in the CW-EPR spectrum appeared (see Figure S3B). This proposes that CW-EPR measurements are insensitive to Atox1 binding at these spin labeling positions.

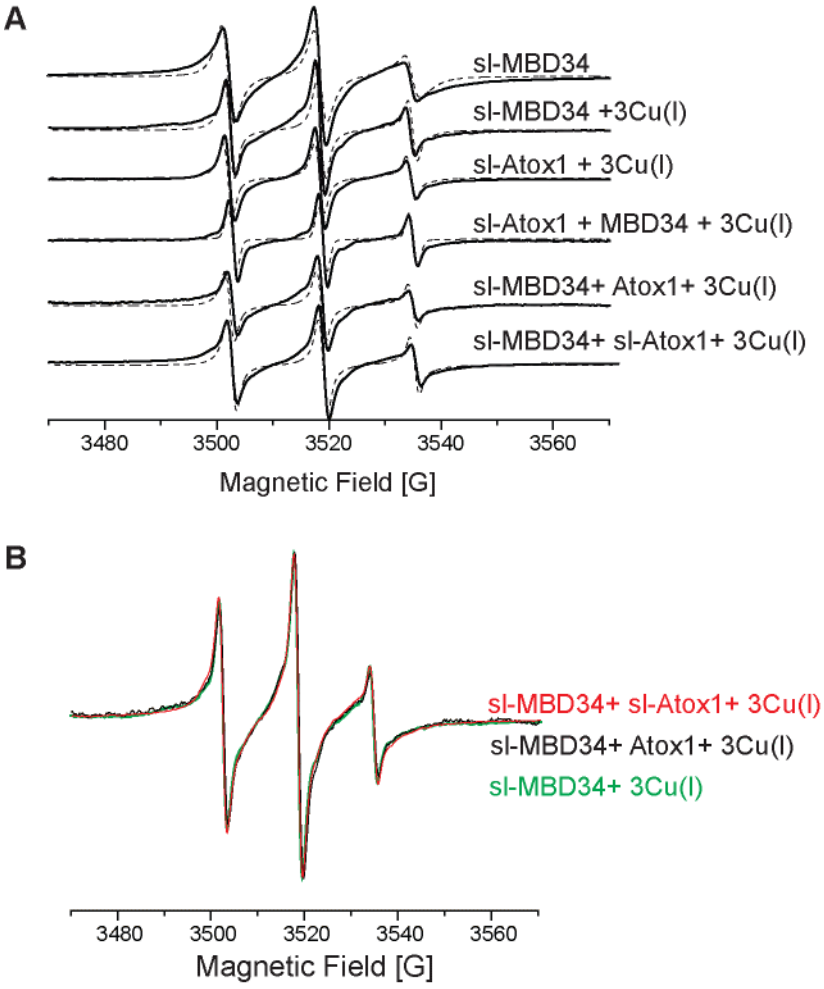

Figure S3: **A**. CW-EPR spectra of spin-labeled WT_MBD3-4 (sl-MBD34), spin-labeled Atox1 (sl-Atox1), with non-spin labeled WT_MBD3-4 (MBD34) and Atox1 in the presence and absence of Cu(I). **B**. The CW-EPR spectra of sl-MBD34 in the presence of Cu(I) (green line), after adding Atox1 to the solution (black line), and after adding sl-Atox1 to the solution (red line).

Cross-linking experiments

To target the interaction between the MBD3-4 and the Atox1 metallochaperone, we performed cross-linking experiments using glutaraldehyde, which reacts with lysine residues. Cross-linking reactions were carried out with 0.1% Glutaraldehyde at RT for 30 minutes in 25 mM Na_2HPO_4, 150 mM NaCl pH = 8 at a protein concentration of 50 μM; the reaction was stopped by the addition of 20 μl of 1 M Tris-HCl pH = 7.4. Figure S4 shows the SDS-PAGE run of Atox1 and MBD3-4 in the presence and absence of Cu(I) ions. Figure S4A shows the cross linking experiment perfomed just on MBD34. It shows that a strong band at around 20-25 KDa corresponds to a MBD3-4 monomer (21.6 KDa). Only at a high concentration is MBD3-4 dimer formed. In the presence of Atox1 (Figure S4B) MBD3-4-Atox1 complex is formed where Atox1 is in a monomeric state, according to the size of the band presented in the gel. Moreover, only one Atox1 monomer forms a complex with MBD3-4, which suggests that either Atox1 interacts with MBD4 or with MBD3. Addition of Cu(I) slightly increases the amount of MBD3-4 dimer (Figure S4C), whereas the interaction between Atox1 and MBD3-4 in the absence and presence of Cu(I) is similar (Figure S4D).

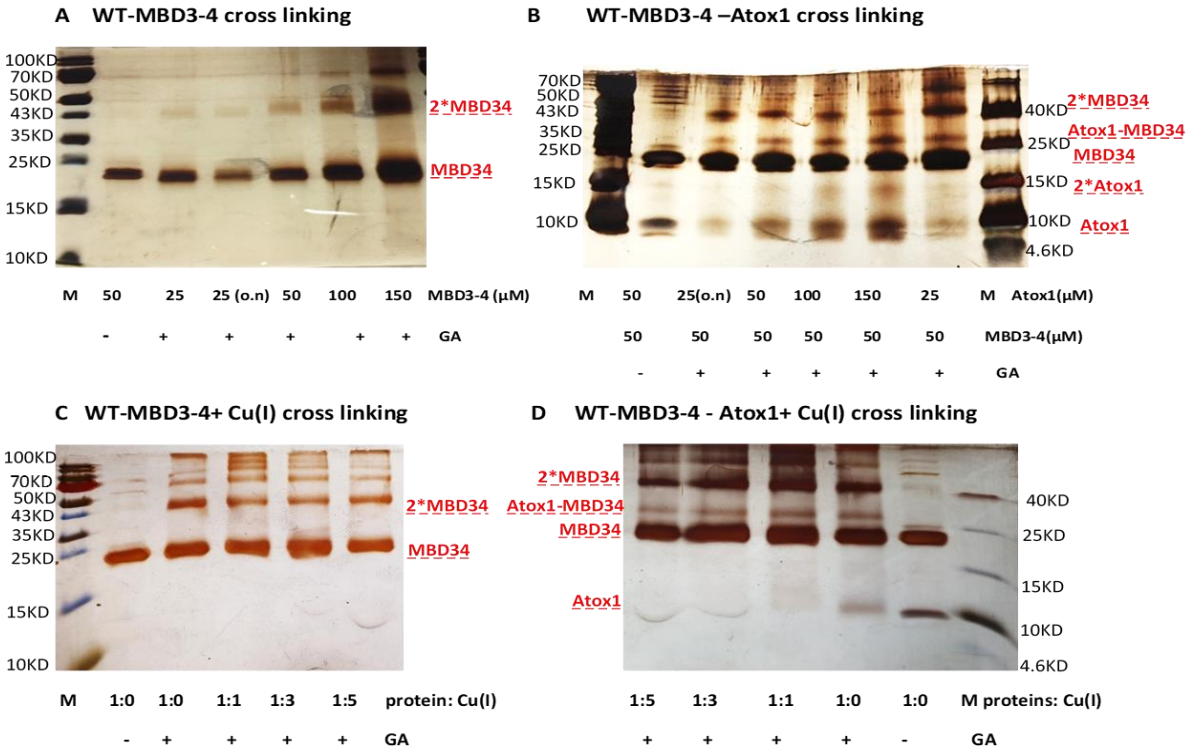

Figure S4: A. Increasing concentrations of WT-MBD3-4 were incubated 30 min or overnight (o.n.) with 0.1% GA at RT. **B**. WT-MBD3-4 (50 µM) was incubated for 30 min with increasing concentrations of Atox1 and then for 30 min or overnight (o.n.) with 0.1% GA at RT. **C**. WT-MBD3-4 (50 µM) was incubated for 30 min with Cu(I) at different ratios and then for 30 min with 0.1% GA at RT. **D.** WT-MBD3-4 and Atox1 (50 µM) were incubated for 30 min with Cu(I) at different ratios and then for 30 min with 0.1% GA at RT.

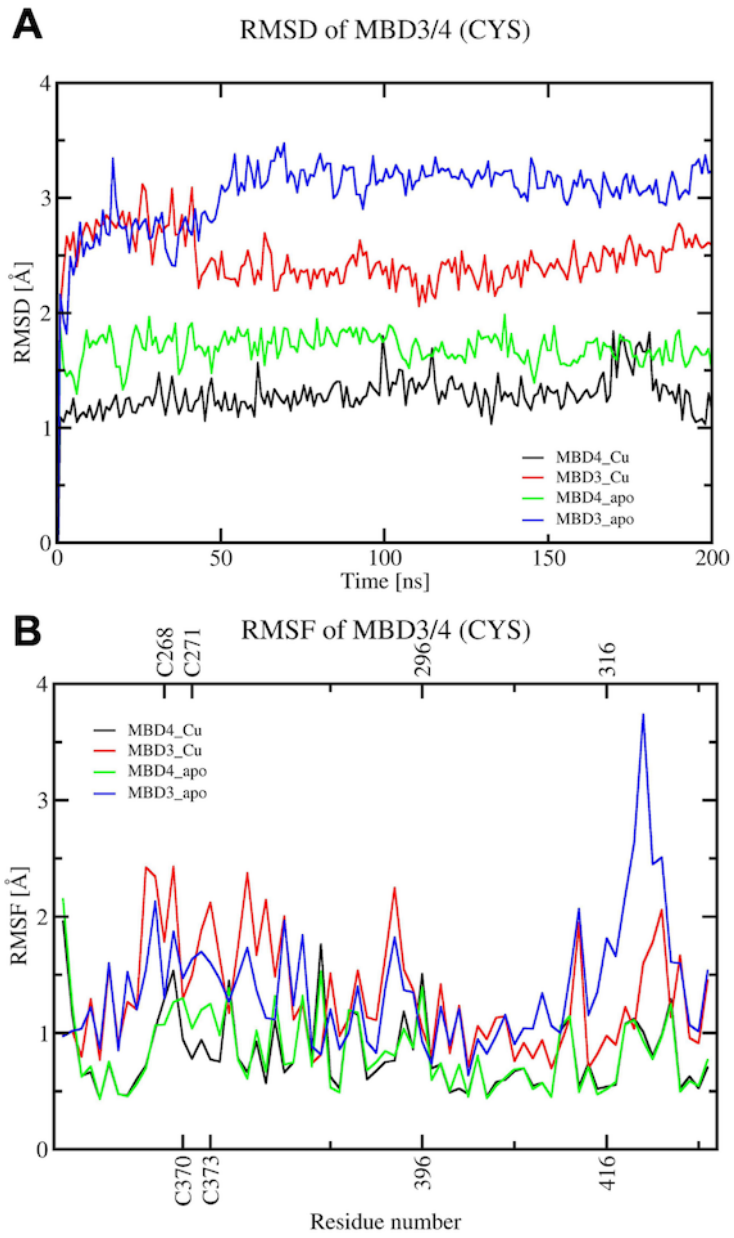

Figure S5: **A.** Root Mean Square Displacement **(**RMSD) plot of WT MBD3 and MBD4 during the 200 ns of classical Molecular dynamics (cMD) simulations (black –holo MBD4; red – holo-MBD3; green – apo MBD4; blue – apo MBD3). **B.** Per residue Root Mean Square Fluctuation (RMSF) plot of MBD3 and 4 during the 200 ns cMD simulations (black – holo MBD4; red – holo MBD3; green – apo MBD4; blue – apo MBD3). Residue numbers for MBD3 and MDB4 are shown on the top and on the bottom, respectively.

Table S2: Relative population of the 5 highest populated clusters (%) for each monomeric system as extracted from classical molecular dynamics trajectories.

Cluster no. / **System**	**1**	**2**	**3**	**4**	**5**
MBD4_CYS_Cu	90.2	7.0	1.1	0.7	0.4
MBD4_CYS_apo	79.9	8.3	5.2	1.8	0.8
MBD3_CYS_Cu	60.0	27.8	11.1	0.9	0.2
MBD3_CYS_apo	50.2	13.5	11.7	7.5	6.4

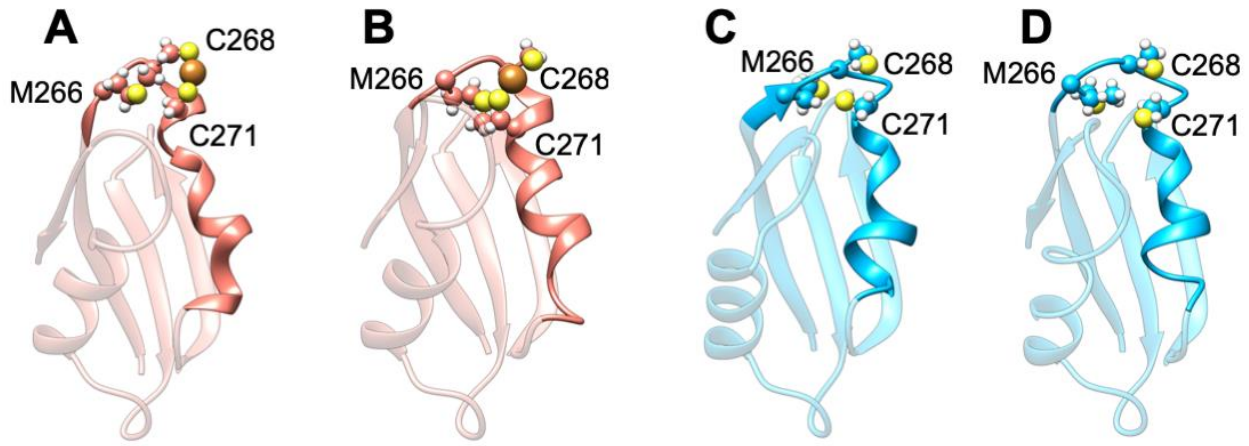

Figure S6: Structures of the second and third highest populated clusters of holo (**A** and **B**) and apo (**C** and **D**) MBD3. Cu(I) is shown as an orange sphere, sulfur atoms are in yellow, and hydrogen atoms in white. Carbon atoms are shown in the color scheme of the protein. The Cu loop and α1 are shown in opaque, whereas the rest of the protein is shown as transparent new cartoons. The relative populations of clusters are reported in Table S2.

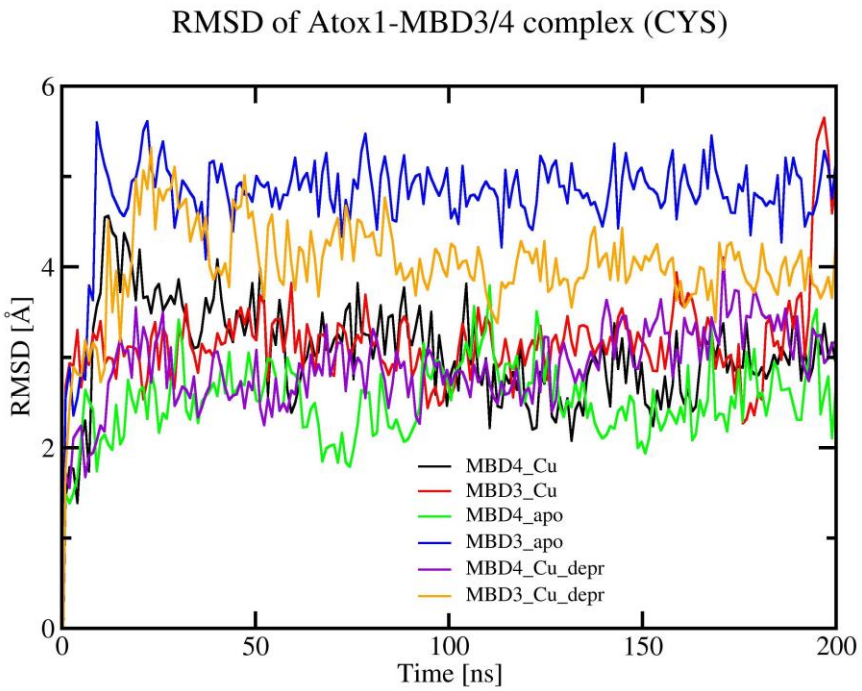

Figure S7: RMSD plot of MBD3/4 in complex with Atox1 during the 200 ns of cMD simulations (black – holo Atox1-MBD4, protonated Cys370 and 373; red – holo Atox1-MBD3, protonated Cys268 and 271; green – apo Atox1-MBD4; blue – apo Atox1-MBD3; violet – holo Atox1-MBD4, deprotonated Cys370 and 373; orange – holo Atox1-MBD3, deprotonated Cys268 and 271).

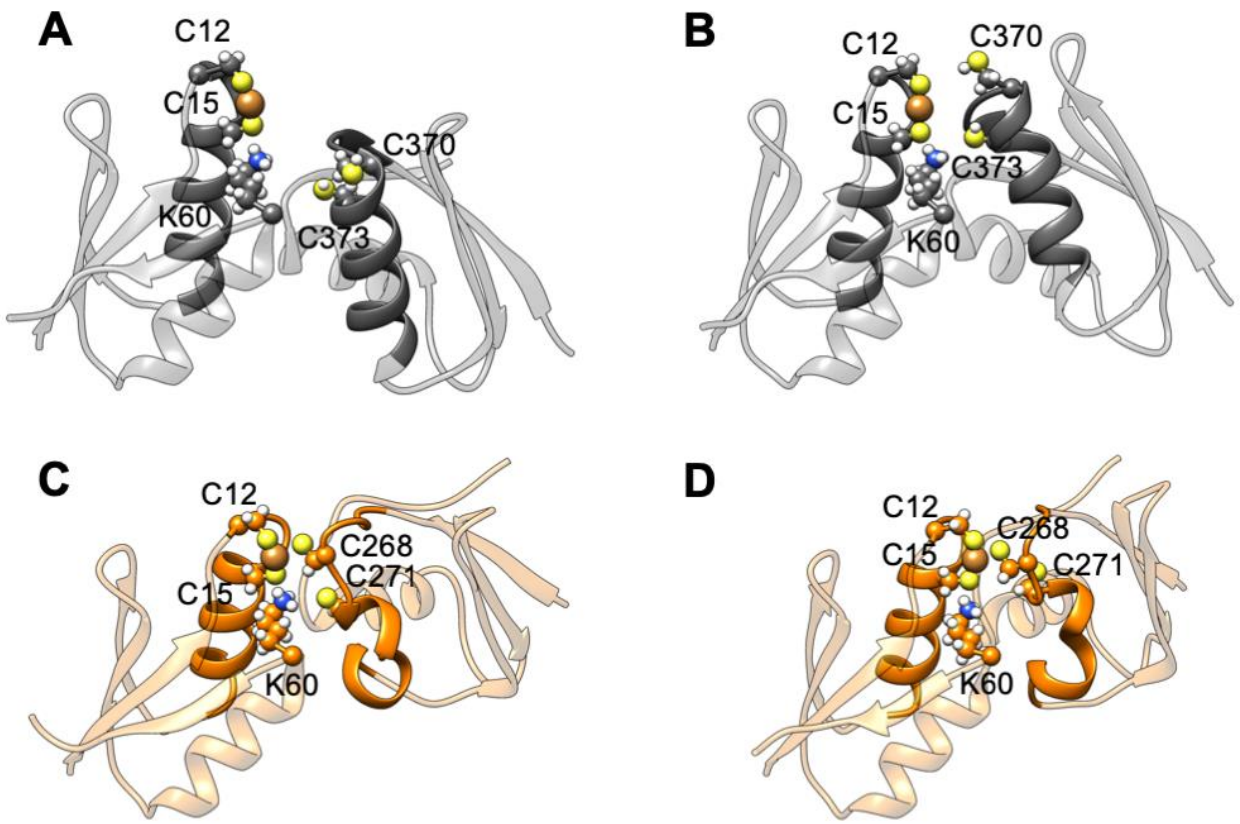

Figure S8: Structures of the second and third highest populated cluster of holo Atox1 in complex with MBD4 (**A** and **B**) and in complex with MBD3 considering Cys268 and Cys271 in the ionized form (**C** and **D**). Cu(I) is shown as an orange sphere, sulfur atoms are in yellow, nitrogen atoms in blue, and hydrogen atoms in white. Carbon atoms are shown in the color scheme of the protein. The Cu loop and α1 in Atox1 and MBD3/4 are shown in opaque, whereas the rest of the protein is depicted as transparent new cartoons. The relative populations of clusters are reported in Table S3.

Table S3: Population of the 5 highest populated clusters (%) for each Atox1-MBD3/4 complex, as extracted from classical molecular dynamics trajectories.

Cluster no. / **System**	**1**	**2**	**3**	**4**	**5**
MBD4_CYS_Cu	48.6	39.0	10.6	1.2	0.1
MBD4_CYS_apo	93.1	3.4	2.5	0.3	0.3
MBD4_CYS_Cu_depr	90.9	6.8	1.0	0.8	0.6
MBD3_CYS_Cu	77.5	7.3	6.8	3.5	3.5
MBD3_CYS_apo	90.1	7.5	1.3	0.2	0.1
MBD3_CYS_Cu_depr	46.1	24.0	23.7	6.2	0.1

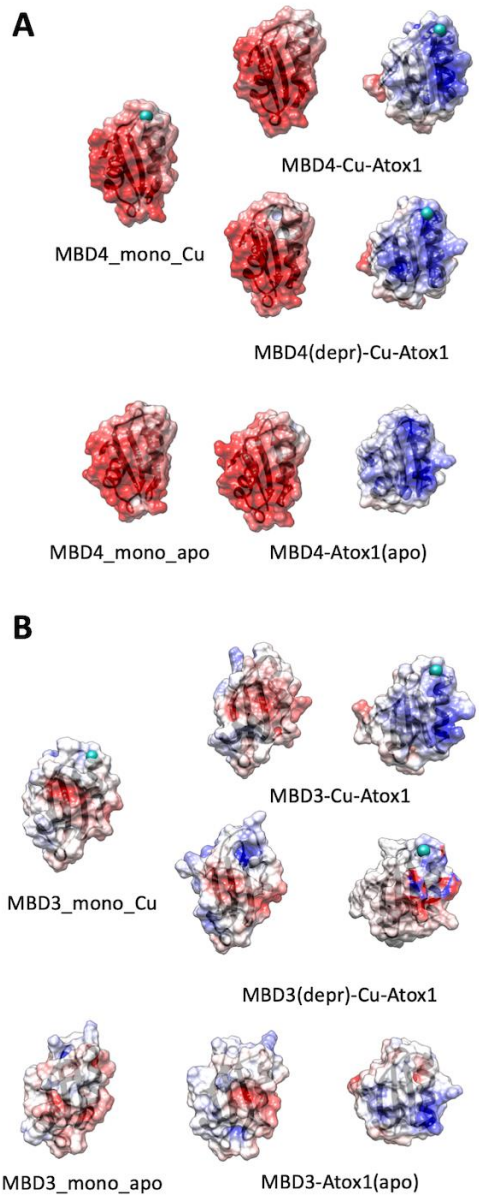

Figure S9: **A.** Electrostatic potential surfaces of holo (MBD4_mono_Cu) and apo (MBD4_mono_apo) MBD4 monomers and Atox1-MBD4 complexes, holo Atox1 in complex with MBD4 with protonated cysteine residues (MBD4-Cu-Atox1), holo Atox1 in complex with MBD4 with deprotonated cysteine residues (MBD4(depr)-Cu-Atox1) and apo Atox1 in complex with MBD4 (MBD4-Atox1(apo). **B.** Electrostatic potential surfaces of holo (MBD3_Cu) and apo (MBD3_apo) MBD3 monomers and Atox1-MBD3 complexes, holo Atox1 in complex with MBD3 with protonated cysteine residues (MBD3-Cu-Atox1), holo Atox1 in complex with MBD3 with deprotonated cysteine residues (MBD3(depr)-Cu-Atox1) and apo Atox1 in complex with MBD3 (MBD3-Atox1(apo). Red on the surface denotes a negative charge and blue a positive charge. Cu(I) is shown as a light blue sphere. The structures of each protein in complexes are shown so that the interacting part of each protein is on the upper part and is facing the viewer.

References:

1. S. Stoll and A. Schweiger, *J. Magn. Reson.*, 2006, **178**, 42-55.